

Adsorption of  $\text{NO}_y$   
on ice

T. Bartels et al.

# The adsorption of nitrogen oxides on crystalline ice

T. Bartels<sup>1</sup>, B. Eichler<sup>1</sup>, P. Zimmermann<sup>1</sup>, H. W. Gäggeler<sup>1,2</sup>, and M. Ammann<sup>1</sup>

<sup>1</sup>Paul Scherrer Institute, CH-5232 Villigen PSI, Switzerland

<sup>2</sup>University of Berne, CH-3012 Bern, Switzerland

Received: 22 February 2002 – Accepted: 9 April 2002 – Published: 16 April 2002

Correspondence to: M. Ammann (markus.ammann@psi.ch)

Title Page

Abstract

Introduction

Conclusions

References

Tables

Figures

◀

▶

◀

▶

Back

Close

Full Screen / Esc

Print Version

Interactive Discussion

© EGS 2002

## Abstract

The partitioning of nitrogen oxides between ice and air is of importance to the ozone budget in the upper troposphere. In the present study, adsorption of nitrogen oxides on ice was investigated at atmospheric pressure using a chromatographic technique with radioactively labelled nitrogen oxides at low concentrations. The measured retentions solely depended on molecular adsorption and were not influenced by dimerisation, formation of encapsulated hydrates on the ice surface, dissociation of the acids, nor by migration into a quasi-liquid layer or grain boundaries. Based on the chromatographic retention and the model of thermo-chromatography, the standard adsorption enthalpy of  $-20 \text{ kJ mol}^{-1}$  for NO,  $-22 \text{ kJ mol}^{-1}$  for  $\text{NO}_2$ ,  $-30 \text{ kJ mol}^{-1}$  for peroxyacetyl nitrate,  $-32 \text{ kJ mol}^{-1}$  for HONO and  $-44 \text{ kJ mol}^{-1}$  for  $\text{HNO}_3$  was calculated. To perform those calculations within the model of thermo-chromatography, the standard adsorption entropy was calculated based on statistical thermodynamics. In this work, two different choices of standard states were applied, and consequently different values of the standard adsorption entropy, of either between  $-39 \text{ J (K mol)}^{-1}$  and  $-45 \text{ J (K mol)}^{-1}$ , or  $-164 \text{ J (K mol)}^{-1}$  and  $-169 \text{ J (K mol)}^{-1}$  for each nitrogen oxide were derived. The standard adsorption enthalpy was identical for both standard adsorption entropies and thus shown to be independent of the choice of standard state. A brief outlook on environmental implications of our findings indicates that adsorption on ice might be an important removal process of  $\text{HNO}_3$ . In addition, it might be of some importance for HONO and peroxyacetyl nitrate and irrelevant for NO and  $\text{NO}_2$ .

## 1. Introduction

Already in the early 70's [Crutzen \(1970\)](#) stressed that nitrogen oxides play a critical role in the atmospheric ozone budget, e.g. in the upper troposphere where an increase in the  $\text{NO}_x$  concentration leads to higher ozone levels ([Jaeglé et al., 1998](#)). Therefore, detailed knowledge of the sources and sinks of nitrogen oxides in the atmosphere is of

## Adsorption of $\text{NO}_y$ on ice

T. Bartels et al.

Title Page

Abstract

Introduction

Conclusions

References

Tables

Figures

◀

▶

◀

▶

Back

Close

Full Screen / Esc

Print Version

Interactive Discussion

**Adsorption of NO<sub>y</sub>  
on ice**

T. Bartels et al.

Title Page

Abstract

Introduction

Conclusions

References

Tables

Figures

◀

▶

◀

▶

Back

Close

Full Screen / Esc

Print Version

Interactive Discussion

© EGS 2002

paramount importance to understand the observed increase of ozone in the free troposphere (Wang et al., 1993) and to model the future composition of the atmosphere. Heterogeneous processes are known to enormously influence the concentration of background gas species. This has become striking clear, ever since the occurrence of the Antarctic ozone hole has been explained (Molina, 1996). Lately, heterogeneous chemistry on ice surfaces, which are one of the main condensed substrates in the upper troposphere and lower stratosphere (Winkler and Trepte, 1998; Heymsfield and Sabin, 1998), has been proposed to explain unusually low nitrogen oxide concentrations observed in cirrus clouds (Reichardt et al., 1996).

In principle, heterogeneous processes can deplete the concentration of gas phase species through uptake on surfaces and subsequent removal processes or increase their concentration through transformation of reservoir species. Yet, for whatever process, the first step is adsorption on the surface. This study aims to evaluate the thermodynamics of adsorption for the reactive nitrogen species NO and NO<sub>2</sub> and the reservoir species HONO, HNO<sub>3</sub> and peroxyacetyl nitrate (PAN) on ice surfaces. Many of the previous studies have focused on the uptake kinetics, whereas the thermodynamics of adsorption are rarely discussed. To our knowledge, only few studies on NO, HONO and HNO<sub>3</sub> adsorption or uptake enthalpies on ice have been published (Sommerfeld et al., 1992; Rieley et al., 1996; Thibert and Dominé, 1998; Tabazadeh et al., 1999; Chu et al., 2000).

We introduce here a method to simultaneously evaluate the adsorption properties of several NO<sub>y</sub> species in synthetic air on ice surfaces. The method combines the advantage of high sensitivity of a radioactive tracer technique with a chromatographic approach, thus enabled us to measure at atmospheric pressure and in a fraction of a monolayer. In brief, radioactively labelled nitrogen oxides in a stream of air or N<sub>2</sub> are fed to a chromatographic column packed with ice spheres. A negative temperature gradient along the column leads to an increasing retention of each species as they are transported in the column. After the experiment, their migration distance in the column is determined by measuring the distribution of radioactivity along the column.

If the model of mobile adsorption is applied, the adsorption enthalpy can be calculated. [Eichler et al. \(2000, 1995\)](#) have shown the feasibility of this approach to derive the standard adsorption enthalpy of  $\text{NO}_y$  on different surfaces and of radon on ice surfaces in previous studies. We will show here that the migration of the nitrogen oxides through the column is neither influenced by dimerisation, migration into a quasi-liquid layer or the grain boundaries, formation of encapsulated hydrates, nor by dissociation of the acids.

## 2. Experimental

### 2.1. Gas phase synthesis

Figure 1 shows the setup of our experiments, which consists of the production of the radioactive nitrogen isotope  $^{13}\text{N}$  ( $t_{1/2} = 10$  min), the synthesis of various  $\text{NO}_y$  species in designated reaction chambers, and the evaluation of their adsorption properties in the chromatographic apparatus. Details of the  $^{13}\text{N}$ -production at Paul Scherrer Institute's Philips Cyclotron and the gas phase synthesis of  $^{13}\text{NO}_2$ ,  $\text{HO}^{13}\text{NO}$  and  $\text{H}^{13}\text{NO}_3$  are described in detail elsewhere ([Ammann, 2001](#)). Briefly, a proton beam ( $1 \mu\text{A}$ ,  $11.1$  MeV) irradiated a  $5 \text{ cm}^3 \text{ s}^{-1}$  flow of 20%  $\text{O}_2$  (99,9995%, Carbagas AG) in He (99,9999%, Carbagas AG). This  $^{16}\text{O}(p, \alpha)^{13}\text{N}$  reaction formed various oxidised  $^{13}\text{N}$ -species inside the gas target, which were reduced to  $^{13}\text{NO}$  by passing them over a molybdenum foil at  $300\text{--}500^\circ\text{C}$ . A transport line of a 80 m polyethylene tube 2 mm in diameter delivered the gas stream to the laboratory. This complete system was placed in a protective argon atmosphere (99,9999%, Carbagas AG) to prevent diffusion of impurities into the gas stream. In the laboratory, the gas flow passed a  $\gamma$ -counter to constantly evaluate the input of  $^{13}\text{N}$ . Afterwards a fraction of the gas stream was diluted with  $\text{N}_2$  (99,9995%, Carbagas AG) or synthetic air and fed to the experiments and a chemiluminescence NO analyzer (CLD, Germany). A molybdenum converter for reduction of  $\text{NO}_y$  to NO was attached to the chemiluminescence analyzer to measure impurities of

## Adsorption of $\text{NO}_y$ on ice

T. Bartels et al.

Title Page

Abstract

Introduction

Conclusions

References

Tables

Figures

◀

▶

◀

▶

Back

Close

Full Screen / Esc

Print Version

Interactive Discussion

**Adsorption of NO<sub>y</sub>  
on ice**

T. Bartels et al.

Title Page

Abstract

Introduction

Conclusions

References

Tables

Figures

◀

▶

◀

▶

Back

Close

Full Screen / Esc

Print Version

Interactive Discussion

© EGS 2002

<sup>14</sup>NO<sub>y</sub>, which come from traces of <sup>14</sup>N<sub>2</sub> in the He- and O<sub>2</sub>-gas. All tubing in the laboratory was kept at room temperature and consisted of perfluoro-alkoxy copolymer (PFA) 4 mm i.d. without any protective gas surrounding them. The diffusion of impurities into the gas stream through PFA, as well as losses and memory effects of the various nitrogen oxides through the column walls are minimal compared to Teflon or polyethylene tubing (Neuman et al., 1999). The work was done under atmospheric pressure and gas flows were controlled by mass flow controllers (Brooks Instruments, The Netherlands) with 1% full scale accuracy.

<sup>13</sup>NO<sub>2</sub> was synthesised by passing the <sup>13</sup>NO over CrO<sub>3</sub> on firebrick support at 30% relative humidity. HO<sup>13</sup>NO was synthesised by passing the <sup>13</sup>NO<sub>2</sub> through a filter impregnated with 100 μl of 1% N-(1-naphthyl)ethylenediamine dihydrochloride (NDA) in methanol-water (10/90) at 30% relative humidity. H<sup>13</sup>NO<sub>3</sub> was produced by photolysis of a <sup>13</sup>NO<sub>2</sub>/H<sub>2</sub>O/O<sub>2</sub> mixture in N<sub>2</sub> at 172 nm. <sup>13</sup>N – PAN was produced through photolysis of acetone at 253 nm in the presence of <sup>13</sup>NO and O<sub>2</sub> (Warneck and Zerbach, 1992). The acetone was dosed to the gas phase by passing a gentle stream of air over solid acetone at 140 K. This saturated gas stream was further diluted prior to entering the photolysis cell. It is very important to work with low acetone concentrations, as in experiments with higher acetone concentrations, the acetone condensed on the ice and column walls, trapped the <sup>13</sup>N – PAN, and consequently hindered its migration. This condensation, which is visible with the naked eyes, was not observed in the experiments described here with the low acetone concentration.

Most syntheses yielded a mixture of several <sup>13</sup>NO<sub>y</sub> as product which, when fed to a column, yielded the adsorption properties of several <sup>13</sup>NO<sub>y</sub> simultaneously. To carry out experiments with only one <sup>13</sup>NO<sub>y</sub> species in the gas phase, a series of selective gas traps were used to scrub all but one species from the gas phase, where possible. The traps, which were designed as cylindrical denuders, were coated with Na<sub>2</sub>CO<sub>3</sub> for absorbing HONO or PAN, a mixture of NDA and KOH (1/1) for NO<sub>2</sub>, NaCl for HNO<sub>3</sub> and Co<sub>2</sub>O<sub>3</sub> for NO (see Kalberer et al. (1996, 1999) for details). Those denuders, in

combination with  $\gamma$ -detectors and the chemiluminescence  $\text{NO}_y$  analyser, were also used to identify and quantify the various  $^{13}\text{NO}_y$  species (Ammann, 2001). In addition, PAN was identified in the gas stream with a GC-ECD (Schrimpf et al., 1995).

## 2.2. Ice preparation and characterisation

5 Deionized water was purified with a Millipore Milli-Q water system to a resistivity  $\leq 0.054 \mu\text{S cm}^{-1}$  and degassed in an ultra-sonic bath. Small droplets, 0.3 - 0.7 mm in diameter, were rapidly frozen in liquid nitrogen. The surface area of the ice spheres was evaluated based on the weight of 100 droplets and an ice density of  $0.85 \text{ g cm}^{-3}$ .  
10 The spheres were annealed in air for at least 12 hours at 258 K in a cold room to allow them to crystallize. The ice spheres were sieved with calibrated sieves (Retsch, Germany) and filled in quartz, Teflon or PFA tubes, which were sealed at each end and stored at 258 K. From the mass of the ice filling and the surface area per gram the surface area per centimeter of the column was calculated, which varied between four and  $10 \text{ cm}^2 \text{ cm}^{-1}$  for the different experiments. During the transport to the laboratory,  
15 the ice columns were cooled to 190 K with solid  $\text{CO}_2$ .

Additionally, BET krypton adsorption measurements were performed to evaluate the surface area of the ice spheres. The measurements were done with a commercially available instrument (Micromeritics, ASAP 2010; U.S.A.), which was equipped with an optional high-vacuum pump. When calculating the adsorbed volume, the instruments  
20 algorithm neglects the temperature profile within the sample holder. This simplification leads in case of measurements of small total surface areas, such as ice surfaces, to an error in the resulting BET surface area. Thus, each measurement was corrected by a reference sample as proposed by Hoff et al. (1998) to eliminate any influence of this simplification and of the sample holder material on the result.

25 In brief, approximately 5 g of the ice spheres were put in a sample holder in the cold room at 258 K, which was transported to the laboratory in a dewar of dry ice, installed at the instrument and immediately immersed in a dewar of liquid nitrogen. In the fol-

## Adsorption of $\text{NO}_y$ on ice

T. Bartels et al.

Title Page

Abstract

Introduction

Conclusions

References

Tables

Figures

◀

▶

◀

▶

Back

Close

Full Screen / Esc

Print Version

Interactive Discussion

---

**Adsorption of NO<sub>y</sub>  
on ice**T. Bartels et al.

---

[Title Page](#)[Abstract](#)[Introduction](#)[Conclusions](#)[References](#)[Tables](#)[Figures](#)[◀](#)[▶](#)[◀](#)[▶](#)[Back](#)[Close](#)[Full Screen / Esc](#)[Print Version](#)[Interactive Discussion](#)

© EGS 2002

lowing automated measurement, the sample holder was evacuated and subsequently dosed with krypton at relative pressures between 0.02 and 0.6. The relative pressure is equal to  $p_i/p^{\text{sat}}$  where  $p_i$  [Pa] is the absolute pressure and  $p^{\text{sat}}$  [Pa] is the saturation pressure. The equilibration interval was set to 10 s, after which the resulting pressure was measured and the adsorbed amount of krypton calculated. Two measurements were performed, one was repeated three times, the second was a single measurement. The free volume of the empty sample holder and the filled sample holder was measured with He prior to each measurement. After the measurement, the ice sample was melted in the sealed sample holder and slowly refrozen with a cooling rate of  $0.5 \text{ K h}^{-1}$ . This procedure generated a smooth ice chunk of identical volume as the ice spheres, but with a negligible surface area. The BET measurements were repeated with this reference sample and the adsorption isotherm of the ice chunk was subtracted from the ice sphere's adsorption isotherm. The resulting adsorption isotherm was used to calculate the BET surface area of the ice spheres.

### 2.3. Thermo-chromatography

A packed ice column was placed in a copper tube along which a negative temperature gradient was established. One end of the copper tube was always immersed into a liquid nitrogen bath, whereas the temperature of the other end, where the gas stream was fed into the column, was varied between 218 K and 250 K with an external cryostat. Prior to each experiment the temperature gradient was measured with a Pt-100 thermo element (MTS, Switzerland) in an empty column. Depending on the temperature at the column entrance and the column length, a temperature gradient between  $-4 \text{ K cm}^{-1}$  and  $-8 \text{ K cm}^{-1}$  was established. Before the experiment the packed columns were placed in the temperature gradient without any gas flow to allow the temperature equilibrium to be reached at any place in the ice column. After that a gas stream containing between 3 ppb and 47 ppb of  $^{13}\text{N}$ -nitrogen oxides was fed to the column for a variable time of 14, 30 or 31 minutes. The flow through the column was controlled with a mass flow controller at the column's exit and varied between  $75 \text{ cm}^3 \text{ min}^{-1}$  and

**Adsorption of NO<sub>y</sub>  
on ice**

T. Bartels et al.

360 cm<sup>3</sup> min<sup>-1</sup>. After the experiment the column was sealed and immersed in an open bath of liquid nitrogen to stop any migration of nitrogen oxides in the column and the distribution of the <sup>13</sup>N-nitrogen oxides in the column was measured, usually exhibiting distinct, symmetric peaks for each NO<sub>y</sub> species. The migration distance, or more precisely, the temperature at this position (denoted as deposition temperature) is the primary observable of the experiment.

#### 2.4. Detection

To deduce the distribution of nitrogen oxides along the column, a coincident  $\gamma$ -counter scanned each column three times. The coincident  $\gamma$ -counter consisted of two Bismuth-Germanate-detectors 3 cm in diameter mounted face to face with a gap of 35 mm. Coincident  $\gamma$ -counting leads to optimum counting efficiency and low background counting rates (less than 1 cts s<sup>-1</sup>), because each decay of <sup>13</sup>N results in two  $\gamma$ -rays in opposite directions to each other. The activity in the column was calculated based on the measured coincident counts and the radioactive decay after the experiment.

To determine the optimum step size of the detectors, the resolution and absolute efficiency of the system, a column was spiked with with point- and broader sources of a <sup>18</sup>F<sup>-</sup> solution of known activity and scanned. The optimum step size turned out to be 0.5 cm, which yielded an accuracy in detection of the peak maximum position of  $\leq 0.5$  cm. The resolution of 3 cm of this arrangement was determined by the detector size, which in addition led to a broadening of the peak base width to 4-6 cm of a point source of  $\leq 0.5$  cm in diameter. With an absolute detector efficiency of 0.0134 observed coincident counts per decay within 1 cm, the detection limit for our experimental setup was  $1 \times 10^5$  molecules <sup>13</sup>N, or  $4 \times 10^{-10}$  mol of total NO<sub>y</sub> (<sup>13</sup>N + <sup>14</sup>N) per centimeter column length.

[Title Page](#)[Abstract](#)[Introduction](#)[Conclusions](#)[References](#)[Tables](#)[Figures](#)[I◀](#)[▶I](#)[◀](#)[▶](#)[Back](#)[Close](#)[Full Screen / Esc](#)[Print Version](#)[Interactive Discussion](#)

© EGS 2002



## 2.5. Derivation of the adsorption enthalpy

The standard adsorption enthalpy was calculated based on the experimentally determined migration distance and the theory of thermo-chromatography (Eichler and Zvára, 1982) using the Maple 6.0 (waterloo maple) software. The detailed formulas are given in the Appendix C, whereas here a brief outline of the calculations is given.

The model of linear chromatography (Eq. 1) describes the position of each species in the column,  $z$  [cm], as function of the time,  $t$  [min], the linear gas velocity,  $u_0$  [cm min<sup>-1</sup>] and the partition function,  $k_i$  [-].

$$\frac{dz}{dt} = \frac{u_0}{1 + k_i} \quad (1)$$

If we substitute  $k_i$  with its thermodynamic definition, and with some further simplifications (see Appendix B) we get Eq. (2), which gives a relation between known experimental factors:  $t_e$  (experimental time),  $g$  (temperature gradient),  $u_0$  (linear gas velocity),  $T_D$  (deposition temperature),  $T_S$  (starting temperature of gradient),  $v$  (open volume in the column),  $a$  (ice surface area in column) and the thermodynamic functions  $\Delta H_{\text{ads}}^0$  (adsorption enthalpy),  $\Delta S_{\text{ads}}^0$  (adsorption entropy),  $T_0$  (standard temperature),  $V/A$  (standard volume to standard surface area),  $R$  (gas constant).

$$\left( t_e + \frac{T_0}{g \cdot u_0} \cdot \ln \frac{T_D}{T_S} \right) \cdot \frac{v \cdot g \cdot u_0}{a \cdot T_0 \cdot \frac{V}{A} \cdot \exp\left(\frac{\Delta S_{\text{ads}}^0}{R}\right)} = \int_{T_S}^{T_D} \frac{1}{T} \cdot \exp\left(\frac{-\Delta H_{\text{ads}}^0}{RT}\right) \quad (2)$$

For each set of experimental parameters,  $\Delta H_{\text{ads}}^0$  was calculated by means of an iteration process with a given  $\Delta S_{\text{ads}}^0$ .  $\Delta S_{\text{ads}}^0$  was calculated based on statistical thermodynamics and the model of mobile adsorption using Eq. (3) with  $h$  (Planck constant),  $k_B$  (Boltzmann constant),  $N_A$  (Loschmidt's number),  $m$  (molar mass) and  $\nu$  (vibrating frequency) of the adsorbed species on the surface, which was assumed to be identical with the phonon frequency of ice (see Appendix D). To our knowledge no experimental

Title Page

Abstract

Introduction

Conclusions

References

Tables

Figures

◀

▶

◀

▶

Back

Close

Full Screen / Esc

Print Version

Interactive Discussion

data about the vibrating frequency  $\nu$  of the solid state of water at temperatures of our experiment exist, a rounded value of  $3 \times 10^{13} \text{ s}^{-1}$  based on the relations of Madelung and Einstein, Lindemann and Debye and data in Hobbs (1974, p. 388) was used (Eichler et al., 2000).

$$\Delta S_{\text{ads}}^0 = R \left[ \ln \left[ \frac{A}{V} \sqrt{\frac{N_A h^2}{2 \pi m k_B T_D}} \right] - 0.5 + \frac{h \nu}{k_B T_D \left( e^{\frac{h \nu}{k_B T_D}} - 1 \right)} \right] \quad (3)$$

### 3. Results and discussion

Figure 2 shows the chromatograms of various nitrogen oxides at low ppb concentrations in ice columns at different experimental settings. Chromatogram A results from exposure of the ice column to  $\text{NO}_2$  (peak at 24 cm) and  $\text{NO}$  (29 cm), B from exposure  $\text{NO}_2$  (24 cm) with some traces of  $\text{HONO}$  (13 cm), C from  $\text{HONO}$  (18 cm) and  $\text{NO}$  (35 cm), D from  $\text{PAN}$  (20 cm) and  $\text{NO}_2$  (25 cm), and E from  $\text{HNO}_3$  (0 cm and 8 cm),  $\text{HONO}$  (18 cm) and  $\text{NO}_2$  (26 cm). It can be clearly seen that each nitrogen oxide species is uniquely retarded in the ice column leading to well defined chromatographic peaks, even if several species are fed to the column simultaneously. The surface concentration of  $\text{NO}_y$  was always at least two orders of magnitude below a monolayer even after accumulation for 30 min, thus condensation was very unlikely in the column. In addition, we did not see a concentration dependence of the migration distance between 3 ppb and 50 ppb  $\text{NO}_y$  in the gas phase, as would be expected for condensational processes. And, the deposition temperatures of the species were much further beyond their boiling point, as we would expect if condensation would have occurred. For example the position of  $\text{NO}_2$  in Fig. 2 B corresponds to a deposition temperature of 144 K, whereas the boiling point is 294 K.

Title Page

Abstract

Introduction

Conclusions

References

Tables

Figures

◀

▶

◀

▶

Back

Close

Full Screen / Esc

Print Version

Interactive Discussion

### 3.1. Mechanistic considerations of the uptake at experimental conditions

The mechanical aspects of adsorption on ice are still under some debate (see Girardet and Toubin, 2001, for a detailed overview). Several possible mechanisms that can be advanced to describe the processes in the chromatographic column are summarized in Fig. 3.

The first question that has to be answered to describe the processes in the column is, whether NO<sub>2</sub> dimerised, as it tends to at low temperatures, or reacted with NO to form N<sub>2</sub>O<sub>3</sub> either in the gas phase or on the surface. For the following consideration, we assumed that the adsorption equilibrium constant describes the partitioning of NO<sub>2</sub> in the column, and chose a typical gas phase concentration of 3 ppb NO<sub>2</sub> and flow rate of 5 cm<sup>3</sup> s<sup>-1</sup>. The concentration of NO<sub>2</sub> first increases due to the temperature decrease at constant pressure up to its maximum value of about 1.3 × 10<sup>11</sup> molecules cm<sup>-3</sup> at 140 K, before it decreases rapidly due to the increasing residence time on the surface. Under these conditions (Atkinson et al., 1999), the extrapolated forward rate constant for formation of N<sub>2</sub>O<sub>4</sub> in the gas phase (Eq. 4) constantly increases from 5 × 10<sup>-2</sup> s<sup>-1</sup> at 250 K to 1.4 × 10<sup>-1</sup> s<sup>-1</sup> at 140 K and decreases again to 10<sup>-2</sup> s<sup>-1</sup> at 120 K.



Obviously, the formation of N<sub>2</sub>O<sub>4</sub> is much slower than the transport of NO<sub>2</sub> in the carrier gas flow, which is almost constant at 0.02 s per cm column length from the column entrance to a position in the column at 140 K. Thus, under the non-steady-state conditions of this chromatographic system the dimerisation is very implausible to occur.

In the colder part of the column, the desorption rate decreases rapidly. It equals 10<sup>8</sup> s<sup>-1</sup> at 250 K, 10<sup>5</sup> s<sup>-1</sup> at 140 K, and 10<sup>2</sup> s<sup>-1</sup> at 120 K. For this estimation, a vibrating frequency,  $\nu$ , of 10<sup>13</sup> s<sup>-1</sup> and an activation energy for desorption, which was assumed to be equal to the adsorption enthalpy, of -22 kJ mol<sup>-1</sup> were chosen (Eq. 5). Once the desorption rate is of the same order of magnitude as the adsorption rate (Eq. 6) the molecules accumulate on the surface and the migration velocity decreases, which

## Adsorption of NO<sub>y</sub> on ice

T. Bartels et al.

Title Page

Abstract

Introduction

Conclusions

References

Tables

Figures

◀

▶

◀

▶

Back

Close

Full Screen / Esc

Print Version

Interactive Discussion

leads to peak formation. The adsorption rate is given by the collision rate on the order of  $10^4 \text{ s}^{-1}$  assuming a sticking coefficient of unity.

$$k_{\text{des}} = \nu \cdot e^{\frac{-\Delta H}{RT}} \quad (5)$$



5 The accumulation could favour dimerisation on the surface, but due to the stronger expected adsorption energies of  $\text{N}_2\text{O}_4$  compared to  $\text{NO}_2$  on the ice surface, a fronting of the peaks should be visible. From the absence of such fronting (see Fig. 2), we conclude that the nitrogen oxides did not dimerise on the surface, nor react to  $\text{N}_2\text{O}_3$ . And from the calculations above, we conclude that  $\text{NO}_2$  did not dimerise in the gas phase and thus the adsorption properties of  $\text{NO}_2$ -monomers were investigated.

10 The second question concerns the processes which determine the retention of the nitrogen oxides in the column. First, we consider  $\text{HNO}_3$ , HONO and PAN, the retention of which is increased at temperatures above 160 K. In the analysis described here we assume a metastable, molecular adsorbed state of these adsorbates on the ice surface ( $\text{NO}_y(\text{ads})$ ), as has been proposed for HCl by [Svanberg et al. \(2000\)](#) based on molecular dynamics simulations. In a subsequent step, the adsorbates may form encapsulated hydrates ( $\text{NO}_y(\text{aq})$ ) within the outermost water bilayer ([Delzeit et al., 1997](#)), which in case of the acids facilitates dissociation ([Packer and Clary, 1995](#)). Recent molecular dynamic simulations by [Bolton and Pettersson \(2000\)](#) confirmed the fact that the ice surface is highly dynamic at temperatures above 180 K. They further indicated that water molecules rapidly (in the order of ns, compared to the species' residence time of ms on the surface) exchange between the upper surface layers. Therefore, we presume that in our experiments not the hydrate formation and dissociation, but the adsorption equilibrium of the molecular species is rate limiting the transport of

15

20

25  $\text{HNO}_3$ , HONO and PAN through the column. The dissociation of acids on ice surfaces, the products of which have been experimentally observed for  $\text{HNO}_3$  by [Zondlo et al. \(1997\)](#), may also rapidly occur directly on the surface ([Svanberg et al., 2000](#); [Clary and](#)

---

**Adsorption of  $\text{NO}_y$   
on ice**T. Bartels et al.

---

Title Page

Abstract

Introduction

Conclusions

References

Tables

Figures

◀

▶

◀

▶

Back

Close

Full Screen / Esc

Print Version

Interactive Discussion

© EGS 2002

Wang, 1997), and thus again not contribute to the retention of HNO<sub>3</sub> and HONO in the column.

In contrast, we assume that NO and NO<sub>2</sub> are exposed to a rather rigid ice surface, as their retention is only enhanced at temperatures below 140 K, and consequently both are not encapsulated by water molecules. Indeed, Uras et al. found molecular HCl at low coverage at 125 K (1998) and showed in a monte carlo simulation that at 110 K NH<sub>3</sub> stays on the ice surface at low coverage and only builds a hydrate capsule within a surface bilayer at high coverage (Uras et al., 2000).

A quasi-liquid layer has been observed at ice surfaces above -24 °C (Bluhm and Salmeron, 1999; Döppenschmidt et al., 1998), and has been used to explain an increased uptake at temperatures approaching the melting point of chemically different species such as NO (Sommerfeld et al., 1992), HNO<sub>3</sub> (Diehl et al., 1998) and SO<sub>2</sub> (Lamb and Clapsaddle, 1989). Although in some of our experiments the nitrogen oxides were exposed to ice at temperatures above -24 °C at the column entrance, the retention is not influenced by diffusion in the quasi-liquid layer. This is nicely illustrated in Fig. 4, which shows two chromatograms of different experimental settings. Similar migration distances of NO<sub>2</sub> were recorded, even when the column entrance was kept at a temperature too low for a quasi-liquid layer to evolve (Fig. 4 A). Obviously, the equilibrium NO<sub>y</sub> (ads) ⇌ NO<sub>y</sub> (qll) shifts so rapidly that the rate limiting factor for transport of the species along the column remains the adsorption equilibrium NO<sub>y</sub> (gas) ⇌ NO<sub>y</sub> (ads). The very small fraction taken up into the quasi-liquid layer, which has not been detected within the relatively short duration of the experiments, did not affect the retention of the molecules. Nevertheless, uptake into the quasi-liquid layer might influence the long-term fate of these species.

For polycrystalline ice, as used in our experiments, an increased uptake at warmer temperatures has been explained by diffusion into the grain boundaries (Huthwelker et al., 2001). In addition, strong acids are known to accumulate in the grain boundaries, as Mulvaney et al. (1988) has shown for H<sub>2</sub>SO<sub>4</sub>. This diffusive process is driven by a strong concentration gradient, and as equilibrium is only reached after hours (Mader,

---

**Adsorption of NO<sub>y</sub>  
on ice**T. Bartels et al.

---

Title Page

Abstract

Introduction

Conclusions

References

Tables

Figures

◀

▶

◀

▶

Back

Close

Full Screen / Esc

Print Version

Interactive Discussion

© EGS 2002

1992), any nitrogen oxide that diffuses into the grain boundaries under our experimental conditions is trapped in the vein system, at least as long as the experiment lasts and thus does not contribute to the peak formation. Furthermore, we note that the surface of the polycrystalline spheres not only consisted of crystalline facies but also of grain boundaries, so that the adsorption enthalpy derived represents an average over all

Concluding, we suggest that the retention of each individual nitrogen oxide solely depends on molecular adsorption processes and thus the theory of thermo-chromatography can very well be applied to our results. We want to state that our current adsorption model does not include changes of the ice surface that are induced by the adsorbate such as restructuring of the ice lattice or vibrational changes (Delzeit et al., 1996).

### 3.2. Standard states

Table 1 shows the standard adsorption enthalpy of the nitrogen oxides examined. To determine the standard adsorption enthalpy based on our experimental findings, the standard adsorption entropy was calculated. The entropy calculations were done with two different standard states, which both yield, as expected, the same standard adsorption enthalpy.

There have been two standard states applied for this work, because for adsorption processes there is no general agreement on the choice of a standard state as for pure gas phase processes. In the literature, two different approaches are usually considered. Eichler and Zvára (1982) arbitrarily set the ratio of  $A/V$  to the value  $1 \text{ cm}^{-1}$ . The advantage of this standard state is its independence of temperature, particle size, and absolute values of  $V$  or  $A$ . Goss (1997) used a standard state introduced by de Boer (1968) and treated the adsorbed species as a two dimensional gas and defined the standard state of that “gas” as state where the average distance of two molecules is identical to the average distance of two molecules in a three dimensional gas phase at standard pressure and temperature. For their calculations, they used the ideal two dimensional gas law which contains the two dimensional pressure  $f [\text{N m}^{-1}]$ . The two

Adsorption of  $\text{NO}_y$   
on ice

T. Bartels et al.

Title Page

Abstract

Introduction

Conclusions

References

Tables

Figures

◀

▶

◀

▶

Back

Close

Full Screen / Esc

Print Version

Interactive Discussion

dimensional gas law allows to calculate a standard surface area of  $6.7 \times 10^{10} \text{ cm}^2$  (A) in analogy to the standard volume of the gas phase of  $2.2 \times 10^4 \text{ cm}^3$  (V).

The two equilibrium constants  $K_p$  can be easily transferred into each other, as Eq. (7) illustrates. Besides the standard surface and volume, the equilibrium constant  $K_p$  depends on the actual surface to volume ratio ( $a/v$ ) in the experimental setup; see Appendix B for further information.

$$\frac{a}{v} \cdot \frac{2.2 \times 10^4}{6.7 \times 10^{10}} \cdot K_p^{01} = \frac{a}{v} \cdot 1 \cdot K_p^{02} \quad (7)$$

### 3.3. Error calculation

Typically, the resulting  $\Delta H_{\text{ads}}^0$  of several experiments showed a standard deviation of about 1% to 3% distributed about the mean. From the experimental setup presented above, it is evident that systematic errors are the main source of uncertainty. To assess this error, calculations based on one particular experiment have been repeated with all factors changed one by one to their possibly largest extent of uncertainty (Table 2). The resulting total difference in  $\Delta H_{\text{ads}}^0$  to the mean value, which varies between 23% and 33%, is given in Table 1 as total error. These total errors agree well with published uncertainties of experiments on adsorption in flow tubes (Fenter et al., 1996).

It can be clearly seen in Table 2 that the most critical input values are those relating on the determination of the deposition temperature and the ice surface (open volume and surface area). The error in the determination of the deposition temperature results mainly from installing the column manually onto the scanner and the resulting inaccuracy of the zero point alignment. The surface areas calculated based on the weight of 100 droplets agreed well with the determination of the radius by sieving. BET measurements of the ice were done to evaluate whether the surface area that is available to adsorption, is of the same size as the geometric surface area. The geometric surface area is the area of a sphere with the same volume as the ice spheres used in our work. In the literature, discrepancy of up to 8 times larger BET surface area per gram

## Adsorption of $\text{NO}_y$ on ice

T. Bartels et al.

Title Page

Abstract

Introduction

Conclusions

References

Tables

Figures

◀

▶

◀

▶

Back

Close

Full Screen / Esc

Print Version

Interactive Discussion

**Adsorption of NO<sub>y</sub>  
on ice**

T. Bartels et al.

Title Page

Abstract

Introduction

Conclusions

References

Tables

Figures

◀

▶

◀

▶

Back

Close

Full Screen / Esc

Print Version

Interactive Discussion

© EGS 2002

sample compared to the external surface area assessed via ESEM pictures, has been observed for ice condensed from the vapour phase (Keyser and Leu, 1993). The BET surface area for two of our ice sphere samples was  $0.006 \text{ m}^2 \text{ g}^{-1}$  and  $0.003 \text{ m}^2 \text{ g}^{-1}$ , respectively, which was of the same order of magnitude as, or even smaller than, the surface area calculated based on the radius of the spheres, being about  $0.007 \text{ m}^2 \text{ g}^{-1}$  and  $0.012 \text{ m}^2 \text{ g}^{-1}$ , respectively. Thus we conclude, that the ice spheres' surface area is not enlarged due to pores or additional microstructures on the surface, and the geometric surface area was used for calculations. Any defects that might have evolved due to the fast freezing of our ice, have probably vanished during the crystallization process at 258 K, or do not influence the adsorption properties of the ice surface. Nevertheless, a high error of 300% was introduced to account for the numerous unknowns such as bulk density of the produced ice, packing density of the column and the accuracy of the method to determine the weight of 100 droplets.

#### 4. Discussion of the standard adsorption enthalpy

Both NO and NO<sub>2</sub> migrate to a temperature of below 140 K in the column and consequently small adsorption enthalpies of  $-20 \text{ kJ mol}^{-1}$  and  $-22 \text{ kJ mol}^{-1}$  are derived. In agreement with our data, Saastad et al. (1993) did not detect any loss of NO in the gas phase above ice frozen from the liquid at temperatures down to 193 K. In contrast, Sommerfeld et al. (1992) found an adsorption enthalpy of  $-11 \text{ kJ mol}^{-1}$  by measuring adsorption isotherms in packed columns down to 200 K using a chromatographic fronting technique. This discrepancy however might be due to the different experimental method and, as Sommerfeld et al. mentioned, a large uncertainty in their measured loss of NO to the ice, as the loss was small compared to the huge background loss of NO on the apparatus' walls. The results of NO<sub>2</sub> adsorption on ice again agree well with findings of Saastad et al. (1993), as in both cases NO<sub>2</sub> did not measurably adsorb on ice at temperatures down to 193 K. Rieley et al. (1996) measured a desorption enthalpy for N<sub>2</sub>O<sub>4</sub> on ice of  $39 \text{ kJ mol}^{-1}$ , which is higher than our findings for NO<sub>2</sub> due to



expected stronger binding interactions.

In our experiments, the adsorption of HONO in the column starts to slow down the migration process at temperatures below 170 K, which qualitatively agrees well with a reversible adsorption of HONO at temperatures of 180–200 K published by Fenter and Rossi (1996). In addition, the HONO standard adsorption enthalpy of  $-32 \text{ kJ mol}^{-1}$  is in excellent agreement with an adsorption enthalpy of  $-33.8 \text{ kJ mol}^{-1}$  reported by Chu et al. (2000).

In all  $\text{HNO}_3$  experiments in this work, two peaks evolved (see Fig. 2 E). The first peak is assigned to an irreversible inclosure of  $\text{HNO}_3$  in the water rime. The riming was only observed in the experiments with  $\text{HNO}_3$  because we had to work at higher relative humidity to generate  $\text{HNO}_3$  from the reaction of  $\text{NO}_2$  with OH on-line. The second peak, at temperatures below 245 K was taken to evaluate the  $\text{HNO}_3$  standard adsorption enthalpy of  $-44 \text{ kJ mol}^{-1}$ . Tabazadeh et al. (1999) published a free enthalpy ( $\Delta G$ ) of  $-59.4 \text{ kJ mol}^{-1}$  for  $\text{HNO}_3$  adsorption and dissociation on ice based on experiments by Abbatt (1997). If we expect the entropy to be negative due to the reduced degrees of freedom of the adsorbed state compared to the gas phase molecule, an upper limit of the enthalpy should be  $-60 \text{ kJ mol}^{-1}$  to fulfill the requirement. This value agrees well with the sublimation enthalpy of  $\text{HNO}_3$  on ice measured by Thibert and Dominé (1998) of  $68 \text{ kJ mol}^{-1}$ . Both values are as expected more negative than our findings, as both describe the enthalpy of adsorption and solvation.

To our knowledge for the first time, the adsorption enthalpy of PAN on ice was found to be  $-30 \text{ kJ mol}^{-1}$ .

The magnitude of the nitrogen oxides' adsorption enthalpies found point to the formation of one to two hydrogen bonds. The strength of a hydrogen bond depends on the capability of an ice surface to act as hydrogen bond donor and the dipole moment of the nitrogen oxide. We expect the capability of the crystalline ice used in this study to form hydrogen bonds, which is determined by the number of free OH groups on the surface, to be sufficient for the submonolayer coverage of nitrogen oxides in this work. First of all, FTIRAS measurements indicated a free OH coverage on crystalline ice to

Adsorption of  $\text{NO}_y$   
on ice

T. Bartels et al.

Title Page

Abstract

Introduction

Conclusions

References

Tables

Figures

◀

▶

◀

▶

Back

Close

Full Screen / Esc

Print Version

Interactive Discussion

**Adsorption of NO<sub>y</sub>  
on ice**

T. Bartels et al.

[Title Page](#)[Abstract](#)[Introduction](#)[Conclusions](#)[References](#)[Tables](#)[Figures](#)[◀](#)[▶](#)[◀](#)[▶](#)[Back](#)[Close](#)[Full Screen / Esc](#)[Print Version](#)[Interactive Discussion](#)

© EGS 2002

be approximately one-sixth of that on amorphous ice (Schaff and Roberts, 1996). And secondly, even after annealing at 258 K the polycrystalline character of the ice spheres used in our work, whose grain boundaries might possess free OH groups, is preserved. Finally, it might even be that despite of the annealing surface defects facilitating free OH groups are present on the surface. Assuming that hydrogen bonding is relevant for adsorption of nitrogen oxides on ice, the overall bond strength of the molecules to the surface should scale with the dipole moment. Figure 5 shows a correlation of some nitrogen oxides' dipole moments and the found standard adsorption enthalpy.

## 5. Atmospheric implications

Table 3 shows the partitioning of nitrogen oxides between ice and air at temperature and surface to volume ratios present in the environment. To calculate the partitioning coefficient (see Eq. 8) at environmental conditions, the standard Gibbs adsorption energy ( $\Delta G_{\text{ads}}^0$ ) was calculated at the temperature of interest based on the standard adsorption enthalpy and entropy from this study (see Eq. 11). The standard Gibbs adsorption enthalpy was in the following transferred to the partitioning coefficient using the actual surface to volume ratio in the environment and the chosen standard state of the enthalpy and entropy calculation (see Eq. 10).

To illustrate the possible influence of adsorption of nitrogen oxides on the gas phase concentrations of NO<sub>x</sub> (see Fig. 3), these back-of-the-envelope calculations were performed with a wide range of environmental conditions. Namely, a high concentration of ice particles of up to 200 cm<sup>-3</sup> typically found in contrails (Schröder et al., 2000), a huge surface area of freshly fallen snow in the arctic and temperate zone (Dominé et al., 2001) or the cold temperatures in the upper troposphere and the typical surface to volume ratio in the clouds (Schröder et al., 2000) were taken. For a detailed description additional factors, such as gas phase and ice diffusion, or additional equilibria following the adsorption have to be included in a more precise model calculation, which is beyond the scope of this work. Nevertheless this rough estimation shows that HNO<sub>3</sub>

**Adsorption of NO<sub>y</sub>  
on ice**

T. Bartels et al.

significantly partitions to the ice phase where ice is abundant, whereas NO and NO<sub>2</sub> do not at all. HONO and PAN might not partition to the ice phase in clouds, but are expected to do so in the snow pack. As the partition coefficient strongly changes with temperature (e. g. for HONO  $k_i \approx 1$  at 230 K and  $k_i \approx 3 \times 10^{-1}$  at 250 K in an arctic environment) emission from or deposition to the snow pack may be expected after strong temperature changes. In addition, uptake on ice might still be a potent removal process, if additional processes follow the adsorption process and thus continuously shift the adsorption equilibrium.

**6. Conclusions**

The retention of nitrogen oxides fed to a chromatographic column filled with ice spheres in synthetic air or nitrogen was investigated at atmospheric pressure and submonolayer coverage. It was argued that the retention was exclusively determined by the equilibrium between a gas phase and a molecularly adsorbed species and not influenced by dimerisation, formation of an encapsulated hydrate on the ice surface, dissociation of the acids, nor by migration into a quasi-liquid layer or grain boundaries.

Based on the migration distance of each nitrogen oxide in the column, the standard enthalpy for molecular adsorption of  $-20 \text{ kJ mol}^{-1}$  for NO,  $-22 \text{ kJ mol}^{-1}$  for NO<sub>2</sub>,  $-30 \text{ kJ mol}^{-1}$  for peroxyacetyl nitrate,  $-32 \text{ kJ mol}^{-1}$  for HONO and  $-44 \text{ kJ mol}^{-1}$  for HNO<sub>3</sub> was calculated. To perform these calculations, a standard state had to be chosen. The standard adsorption enthalpy proved to be independent of that choice, and is thus an ideal value for comparison of adsorption energies with other groups. An error analysis revealed the actual surface area of the ice as major source of systematic uncertainty of the standard adsorption calculations. Nevertheless, the total error associated with the reported standard adsorption enthalpy is less than 33%.

A brief outlook on environmental implications of our findings for exemplary conditions in contrails, cirrus clouds, as well as arctic and temperate zone snow packs indicated that adsorption on ice might be an important removal process of HNO<sub>3</sub>, of some im-

[Title Page](#)[Abstract](#)[Introduction](#)[Conclusions](#)[References](#)[Tables](#)[Figures](#)[◀](#)[▶](#)[◀](#)[▶](#)[Back](#)[Close](#)[Full Screen / Esc](#)[Print Version](#)[Interactive Discussion](#)

© EGS 2002

portance for HONO and peroxyacetyl nitrate and irrelevant for NO and NO<sub>2</sub>.

*Acknowledgements.* The authors thank E. Rössler, M. Birrer and D. Piguet for continuing support of our work, F. Geiger for help with the BET measurements and the staff of PSI Accelerator Facilities for the beam generation. This work is part of the EU project CUT-ICE (EVK2-CT1999-00005) funded by the Swiss Federal Office for Education and Science (99.00491-2). We would also like to thank all CUT-ICE partners for the discussions during the CUT-ICE meetings.

**ACPD**

2, 431–468, 2002

---

**Adsorption of NO<sub>y</sub>  
on ice**

T. Bartels et al.

---

Title Page

Abstract

Introduction

Conclusions

References

Tables

Figures

◀

▶

◀

▶

Back

Close

Full Screen / Esc

Print Version

Interactive Discussion

© EGS 2002

## Appendix A: Notation

Symbol	Explanation		Unit
$S$	entropy		$\text{J (K mol)}^{-1}$
$H$	enthalpy		$\text{J (K mol)}^{-1}$
$U$	inner energy		$\text{J (K mol)}^{-1}$
$U(0)$	zero inner energy		$\text{J (K mol)}^{-1}$
$q$	molecular partition function		–
$Q$	molar partition function		–
$T$	temperature		K
$T_D$	deposition temperature		K
$u$	linear gas velocity		$\text{cm min}^{-1}$
$u_0$	linear gas velocity at standard temp.		$\text{cm min}^{-1}$
$a$	surface area		$\text{cm}^2$
$v$	volume		$\text{cm}^3$
$p$	pressure		$\text{N m}^{-2}$
$f$	two dimensional pressure		$\text{N m}^{-1}$
$A$	standard surface area		$\text{cm}^2$
$V$	standard volume		$\text{cm}^3$
$p^0$	standard pressure	1	$\times 10^5 \text{ N m}^{-2}$
$f^0$	standard two dimensional pressure	3.38	$\times 10^{-2} \text{ N m}^{-1}$
$M$	molecular mass		kg
$m$	molar mass		$\text{kg mol}^{-1}$
$n$	number of molecules		–
$\nu$	vibrating frequency		$\text{s}^{-1}$
$N_A$	Loschmidt's number	$6.02285 \times 10^{23}$	$\text{mol}^{-1}$
$k_B$	Boltzmann constant	$1.38066 \times 10^{-23}$	$\text{J K}^{-1}$
$h$	Planck constant	$6.62618 \times 10^{-34}$	J s
$R$	gas constant	8.31441	$\text{J (K mol)}^{-1}$

## Adsorption of $\text{NO}_y$ on ice

T. Bartels et al.

Title Page

Abstract

Introduction

Conclusions

References

Tables

Figures

◀

▶

◀

▶

Back

Close

Full Screen / Esc

Print Version

Interactive Discussion

## Appendix B: Partitioning coefficient, adsorption equilibrium constant and standard states

At low concentrations the partitioning of each species in the chromatographic column, or in any two phase system, can be described by the partition coefficient (Eq. 8), which gives a relation of the total number of adsorbed and gaseous species.

$$k_i = \frac{n^{\text{ads}}}{n^{\text{gas}}} [-] \quad (8)$$

This partition can be described by the adsorption equilibrium constant, which accounts for the influence of the actual surface to volume ratio on the column (Eq. 9).

$$\begin{aligned} K_c &= \frac{n^{\text{ads}}/a}{n^{\text{gas}}/v} [cm] \\ &= k_i \cdot \frac{v}{a} [cm] \end{aligned} \quad (9)$$

To perform thermodynamical calculations, the adsorption equilibrium constant ( $K_c$ ) has to be transferred into the dimensionless standard equilibrium constant ( $K_p$ ), as can be seen in Eq. (10).

$$\begin{aligned} K_p &= \frac{f/f^0}{p/p^0} [-] \\ &= \frac{n^{\text{ads}}/a \cdot RT \cdot p^0}{n^{\text{gas}}/v \cdot RT \cdot f^0} [-] \\ &= k_i \cdot \frac{v}{a} \cdot \frac{A}{V} [-] \end{aligned} \quad (10)$$

The advantage of the standard adsorption equilibrium constant ( $K_p$ ) is, that it can be expressed in terms of the standard adsorption entropy and enthalpy (Eq. 11), which

### Adsorption of NO<sub>y</sub> on ice

T. Bartels et al.

Title Page

Abstract

Introduction

Conclusions

References

Tables

Figures

◀

▶

◀

▶

Back

Close

Full Screen / Esc

Print Version

Interactive Discussion

can be regarded as independent of temperature.

$$-RT \ln K_p = \Delta H_{\text{ads}}^0 - T \Delta S_{\text{ads}}^0 \quad (11)$$

### Appendix C: The transport model and enthalpy calculations

The calculation of the standard adsorption enthalpy within the model of thermo-chromatography has been described by [Eichler and Zvára \(1982\)](#) in great detail. The transport of a species along the chromatographic column at low concentrations is given by Eq. (12).

$$\frac{dz}{dt} = \frac{u_0}{1 + K_f} \quad (12)$$

If a linear temperature gradient along the column (Eq. 13) is given,

$$T = T_s - g \cdot z, \quad (13)$$

Eq. (12) yields

$$t = -\frac{1}{g} \int_{T_s}^{T_D} \frac{1 + \frac{a}{v} \cdot \frac{V}{A} K_p(T)}{u(T)} dT. \quad (14)$$

Neglecting the change in gas pressure along the column, we have

$$u(T) = \frac{u_0 \cdot T}{T_0} [cm s^{-1}]. \quad (15)$$

Assuming that  $\Delta H_{\text{ads}}^0$  and  $\Delta S_{\text{ads}}^0$  are independent of temperature, and substituting Eqs. (10), (11) and (15) in Eq. (14), we obtain Eq. (16), which can be solved by an iteration process, if  $\Delta S_{\text{ads}}^0$  is known.

$$\left( t + \frac{T_0}{g \cdot u_0} \cdot \ln \frac{T_D}{T_s} \right) \cdot \frac{v \cdot g \cdot u_0}{a \cdot T_0 \cdot \frac{V}{A} \cdot \exp\left(\frac{\Delta S_{\text{ads}}^0}{R}\right)} = \int_{T_s}^{T_D} \frac{1}{T} \cdot \exp\left(\frac{-\Delta H_{\text{ads}}^0}{RT}\right) \quad (16)$$

## Adsorption of NO<sub>y</sub> on ice

T. Bartels et al.

Title Page

Abstract

Introduction

Conclusions

References

Tables

Figures

◀

▶

◀

▶

Back

Close

Full Screen / Esc

Print Version

Interactive Discussion

## Appendix D: Entropy calculations

Statistical thermodynamics allow to very precisely calculate the absolute entropy based on the partition functions. In the following we will calculate the change in entropy during adsorption as the difference of the absolute entropy of a molecule in the gas phase and of the molecule in the adsorbed state (Eq. 17).

$$\Delta S_{\text{ads}} = S_{\text{ads}} - S_{\text{gas}} \quad (17)$$

Each entropy term can be calculated based on the molar partition function, Eq. (18). Using Stirling's approximation and  $R = k_B \cdot N_A$  the partition function can be written as the molecular partition function (Eq. 19) for the canonical ensemble (Eq. 20).

$$S = \frac{\{U - U(0)\}}{T} + k_B \cdot \ln Q \quad (18)$$

$$S = \frac{\{U - U(0)\}}{T} + nR \cdot \ln \{\ln q - \ln N_A + 1\} \quad (19)$$

$$Q = q^n / n! \quad (20)$$

The inner energy,  $U - U(0)$ , can itself be calculated based on the partition functions (Eq. 21).

$$\begin{aligned} U - U(0) &= -n \frac{\delta \ln q}{\delta kT} \\ &= -n k_B T^2 \frac{\delta \ln q}{\delta T} \end{aligned} \quad (21)$$

The partition function is simply calculated based on the molecule's translational (trans), rotational (rot), vibrational (vib) and electrical (el) degrees of freedom (Eq. 22).

$$q^{\text{tot}} = q^{\text{trans}} \cdot q^{\text{rot}} \cdot q^{\text{vib}} \cdot q^{\text{el}} \quad (22)$$

The adsorbed state is defined by a large mobility of the adsorbed molecules on the surface and a vibrating mode perpendicular to the surface. The molecule only loses

Title Page

Abstract

Introduction

Conclusions

References

Tables

Figures

◀

▶

◀

▶

Back

Close

Full Screen / Esc

Print Version

Interactive Discussion



one translational degree of freedom and gains one vibrational degree of freedom during adsorption. As internal vibrations, rotations and the electronic configuration do not change and thus do not contribute to the adsorption entropy, we can calculate the partition function solely based on the translational and vibrational partition function.

5 The translational partition function is calculated based on a particle-in-the-box as

$$q^{\text{trans}} = V \cdot \left( \frac{2 \pi m k_B T}{h^2} \right)^{3/2} \quad (23)$$

for the three dimensional state and as

$$q^{\text{trans}} = A \cdot \left( \frac{2 \pi m k_B T}{h^2} \right) \quad (24)$$

10 for the two dimensional (adsorbed) state. The vibrational partition function for one mode is given by

$$q^{\text{vib}} = \frac{e^{-\frac{h\nu}{2kT}}}{1 - e^{-\frac{h\nu}{k_B T}}} \quad (25)$$

The vibrating frequency ( $\nu$ ) of the molecule in the adsorbed state is considered to be similar to the phonon frequency of ice. Since to our knowledge no experimental data about the vibrating frequency of the solid state of water exist at these temperatures, a rounded value of  $3 \times 10^{13} \text{ s}^{-1}$  based on the relations of Madelung and Einstein, Lindemann and Debye and data in [Hobbs \(1974, p. 388\)](#) was used.

Using Eqs.(21) and (23) to calculate the contribution of the inner energy to the entropy yields

$$\frac{U - U(0)}{T} = \frac{3}{2} k_B N_A \quad (26)$$

20 for the molecules in the gas phase. Similarly, for the adsorbed state based on Eqs. (21),

**Adsorption of NO<sub>y</sub> on ice**

T. Bartels et al.

Title Page

Abstract

Introduction

Conclusions

References

Tables

Figures

◀

▶

◀

▶

Back

Close

Full Screen / Esc

Print Version

Interactive Discussion

(24) and (25), we get

$$\frac{U - U(0)}{T} = k_B N_A + k_B N_A \cdot \frac{h\nu}{2k_B T} + \frac{N_A k_B \cdot h\nu}{k_B T \cdot \left(e^{\frac{h\nu}{k_B T}} - 1\right)}. \quad (27)$$

Using Eqs. (17), (19), and (23-27), we finally get the standard adsorption entropy

$$\begin{aligned} \Delta S_{\text{ads}}^0 = & k_B N_A - \frac{3}{2} k_B N_A + k_B N_A \cdot \frac{h\nu}{2k_B T} + \frac{N_A k_B \cdot h\nu}{k_B T \cdot \left(e^{\frac{h\nu}{k_B T}} - 1\right)} \\ & + N_A k_B \left[ \ln \left( \frac{A}{V} \sqrt{\frac{h^2}{2\pi m k_B T}} \right) + \ln e^{-\frac{h\nu}{2k_B T}} - \ln \left( 1 - e^{-\frac{h\nu}{k_B T}} \right) \right] \end{aligned} \quad (28)$$

and with  $\ln \left( 1 - e^{-\frac{h\nu}{k_B T}} \right)$  being approximately 0, Eq. (28) finally yields Eq. (29), which was used for calculations in this work.

$$\Delta S_{\text{ads}}^0 = R \left[ \ln \left[ \frac{A}{V} \sqrt{\frac{N_A h^2}{2\pi m k_B T_D}} \right] - 0.5 + \frac{h\nu}{k_B T_D \left( e^{\frac{h\nu}{k_B T_D}} - 1 \right)} \right] \quad (29)$$

## References

- Abbatt, J. P. D.: Interaction of HNO<sub>3</sub> with water-ice surfaces at temperatures of the free troposphere, *Geophysical Research Letters*, 24, 1479–1482, 1997. [447](#)
- Ammann, M.: Using <sup>13</sup>N as tracer in heterogeneous atmospheric chemistry experiments, *Radiochimica Acta*, 89, 831–838, 2001. [434](#), [436](#)
- Atkinson, R., Baulch, D. L., Cox, R. A., Hampson, R. F., Kerr, J. A., Rossi, M. J., and Troe, J.: Summary of evaluated kinetic and photochemical data for atmospheric chemistry, <http://www.iupac-kinetic.ch.cam.ac.uk>, 1999. [441](#)

[Title Page](#)
[Abstract](#)
[Introduction](#)
[Conclusions](#)
[References](#)
[Tables](#)
[Figures](#)
[◀](#)
[▶](#)
[◀](#)
[▶](#)
[Back](#)
[Close](#)
[Full Screen / Esc](#)
[Print Version](#)
[Interactive Discussion](#)

© EGS 2002

**Adsorption of NO<sub>y</sub>  
on ice**

T. Bartels et al.

Title Page

Abstract

Introduction

Conclusions

References

Tables

Figures

◀

▶

◀

▶

Back

Close

Full Screen / Esc

Print Version

Interactive Discussion

© EGS 2002

Bluhm, H. and Salmeron, M.: Growth of nanometer thin ice films from water vapor studied using scanning polarization force microscopy, *Journal of Physical Chemistry*, 111, 6947–6954, 1999. [443](#)

Bolton, K. and Pettersson, J. B. C.: A molecular dynamics study of the long-time ice Ih surface dynamics, *Journal of Physical Chemistry B*, 104, 1590–1595, 2000. [442](#)

Chu, L., Diao, G., and Chu, L. T.: Heterogeneous interaction and reaction of HONO on ice films between 173 and 230 K, *Journal of Physical Chemistry A*, 104, 3150–3158, 2000. [433](#), [447](#)

Clary, D. C. and Wang, L. C.: Influence of surface defects on the adsorption of HCl on ice, *Journal of the Chemical Society-Faraday Transactions*, 93, 2763–2767, 1997. [442](#)

Crutzen, P. J.: The influence of nitrogen oxides on the atmospheric ozone content, *Quarterly Journal of the Royal Meteorological Society*, 96, 320–325, 1970. [432](#)

de Boer, J. H.: *The Dynamical Character of Adsorption*, Clarendon Press, Oxford, 1968. [444](#)

Delzeit, L., Devlin, M. S., Rowland, B., Devlin, J. P., and Buch, V.: Adsorbate-induced partial ordering of the irregular surface and subsurface of crystalline ice, *Journal of Physical Chemistry*, 100, 10 076–10 082, 1996. [444](#)

Delzeit, L., Powell, K., Uras, N., and Devlin, J. P.: Ice surface reactions with acids and bases, *Journal of Physical Chemistry B*, 101, 2327–2332, 1997. [442](#)

Diehl, K., Mitra, S. K., and Pruppacher, H. R.: A laboratory study on the uptake of HCl, HNO<sub>3</sub> and SO<sub>2</sub> gas by ice crystals and the effect of these gases on the evaporation rate of the crystals, *Atmospheric Research*, 48, 235–244, 1998. [443](#)

Dominé, F., Cabanes, A., Taillandier, A.-S., and Legagneux, L.: Specific surface area of snow samples determined by CH<sub>4</sub> adsorption at 77 K and estimated by optical microscopy and scanning electron microscopy, *Environmental Science and Technology*, 35, 771–780, 2001. [448](#)

Döppenschmidt, A., Kappl, M., and Butt, H.-J.: Surface properties of ice studied by atomic force microscopy, *Journal of Physical Chemistry B*, 102, 7813–7819, 1998. [443](#)

Eichler, B. and Zvára, I.: Evaluation of the enthalpy of adsorption from thermochromatographical data, *Radiochimica Acta*, 30, 233–238, 1982. [439](#), [444](#), [453](#)

Eichler, B., Baltensperger, U., Ammann, M., Jost, D. T., Gäggeler, H. W., and Türlér, A.: Thermochromatographic investigation of <sup>13</sup>N-labelled nitrous gases and of fission noble gases at low temperatures, *Radiochimica Acta*, 68, 41–49, 1995. [434](#)

Eichler, B., Zimmermann, H. P., and Gäggeler, H.: Adsorption of radon on ice surfaces, *Journal of Physical Chemistry A*, 104, 3126–3131, 2000. [434](#), [440](#)

**Adsorption of NO<sub>y</sub>  
on ice**

T. Bartels et al.

Title Page

Abstract

Introduction

Conclusions

References

Tables

Figures

◀

▶

◀

▶

Back

Close

Full Screen / Esc

Print Version

Interactive Discussion

© EGS 2002

- Fenter, F. F. and Rossi, M. J.: Heterogeneous kinetics of HONO on H<sub>2</sub>SO<sub>4</sub> solutions and on ice: Activation of HCl, *Journal of Physical Chemistry*, 100, 13 765–13 775, 1996. [447](#)
- Fenter, F. F., Caloz, F., and Rossi, M. J.: Heterogeneous kinetics of N<sub>2</sub>O<sub>5</sub> uptake on salt, with a systematic study of the role of surface presentation (for N<sub>2</sub>O<sub>5</sub> and HNO<sub>3</sub>), *Journal of Physical Chemistry*, 100, 1008–1019, 1996. [445](#)
- Girardet, C. and Toubin, C.: Molecular atmospheric pollutant adsorption on ice: a theoretical survey, *surface science reports*, 44, 159–238, 2001. [441](#)
- Goss, K.-U.: Conceptual model for the adsorption of organic compounds from the gas phase to liquid and solid surfaces, *Environmental Science and Technology*, 31, 3600–3605, 1997. [444](#)
- Heymsfield, A. J. and Sabin, R. M.: Cirrus crystal nucleation by homogeneous freezing of solution droplets, *Journal of Atmospheric Research*, 46, 2252–2264, 1998. [433](#)
- Hobbs, P. V.: *Ice physics*, Clarendon Press, Oxford, 1974. [440](#), [455](#)
- Hoff, J. T., Gregor, D., Mackay, D., Wania, F., and Jia, C. Q.: Measurement of the specific surface area of snow with the nitrogen adsorption technique, *Environmental Science and Technology*, 32, 58–62, 1998. [436](#)
- Huthwelker, T., Lamb, D., Baker, M., Swanson, B., and Peter, T.: Uptake of SO<sub>2</sub> by polycrystalline water ice, *Journal of Colloid and Interface Science*, 238, 174–159, 2001. [443](#)
- Jaeglé, L., Jacob, D. J., Brune, W. H., Tan, D., Faloon, I. C., Weinheimer, A. J., Ridley, B. A., Campos, T. L., and Sachse, G. W.: Sources of HO<sub>x</sub> and production of ozone in the upper troposphere over the united states, *Geophysical Research Letters*, 25, 1709–1712, 1998. [432](#)
- Kalberer, M., Tabor, K., Ammann, M., Parrat, Y., Weingartner, E., Piguet, D., Rössler, E., Jost, D. T., Türlér, A., Gäggeler, H. W., and Baltensperger, U.: Heterogeneous chemical processing of <sup>13</sup>NO<sub>2</sub> by monodisperse carbon aerosols at very low concentrations, *Journal of Physical Chemistry*, 100, 15 487–15 493, 1996. [435](#)
- Kalberer, M., Ammann, M., Arens, F., Gäggeler, H. W., and Baltensperger, U.: Heterogeneous formation of nitrous acid (HONO) on soot aerosol particles, *Journal of Geophysical Research*, 104, 13 825–13 832, 1999. [435](#)
- Keyser, L. F. and Leu, M.-T.: Surface areas and porosities of ices used to simulate stratospheric clouds, *Journal of Colloid and Interface Science*, 155, 137–145, 1993. [446](#)
- Lamb, D. and Clapsaddle, C.: The sorption of SO<sub>2</sub> on ice at temperatures between -30°C and -5°C, *Geophysical Research Letters*, 16, 1173–1176, 1989. [443](#)

---

**Adsorption of NO<sub>y</sub>  
on ice**

---

T. Bartels et al.

---

Title Page

Abstract

Introduction

Conclusions

References

Tables

Figures

◀

▶

◀

▶

Back

Close

Full Screen / Esc

Print Version

Interactive Discussion

© EGS 2002

- Lide, D. R.: (Ed) Handbook of Chemistry and Physics, CRC Press, New York, 82 edn., 2001–2002. [468](#)
- Mader, H. M.: The thermal behaviour of the water-vein system in polycrystalline ice, *Journal of Glaciology*, 38, 359–374, 1992. [443](#)
- 5 Molina, M. J.: Polar ozone depletion (nobel lecture), *Angewandte Chemie-International Edition in English*, 35, 1778–1785, 1996. [433](#)
- Mulvaney, R., Wolff, E. W., and Oates, K.: Sulphuric acid at grain boundaries in antarctic ice, *Nature*, 331, 247–249, 1988. [443](#)
- 10 Neuman, J. A., Huey, L. G., Ryerson, T. B., and Fahey, D. W.: Study of inlet materials for sampling atmospheric nitric acid, *Environmental Science and Technology*, 33, 1133–1136, 1999. [435](#)
- Packer, M. J. and Clary, D. C.: Interaction of HCl with water clusters: (H<sub>2</sub>O)<sub>n</sub>HCl, n = 1 – 3, *Journal of Physical Chemistry*, 99, 14 323–14 333, 1995. [442](#)
- 15 Reichardt, J., Ansmann, A., Serwazi, M., Weitkamp, C., and Michaelis, W.: Unexpectedly low ozone concentration in midlatitude tropospheric ice clouds: A case study, *Geophysical Research Letters*, 23, 1929–1932, 1996. [433](#)
- Rieley, H., McMurray, D. P., and Haq, S.: Adsorption and photochemistry of dinitrogen tetroxide on low temperature ice layers, *Journal of The Chemical Society - Faraday Transactions*, 92, 933–939, 1996. [433](#), [446](#)
- 20 Saastad, O. W., Ellermann, T., and Nielsen, C. J.: On the adsorption of NO and NO<sub>2</sub> on cold H<sub>2</sub>O/H<sub>2</sub>SO<sub>4</sub> surfaces, *Geophysical Research Letters*, 20, 1191–1193, 1993. [446](#)
- Schaff, J. E. and Roberts, J. T.: Toward an understanding of the surface chemical properties of ice: Differences between the amorphous and crystalline surfaces, *Journal of Physical Chemistry*, 100, 14 151–14 160, 1996. [448](#)
- 25 Schrimpf, W., Müller, K. P., Johnen, F. J., Lienaerts, K., and Rudolph, J.: An optimized method for airborne peroxyacetyl nitrate (PAN) measurements, *Journal of Atmospheric Chemistry*, 22, 303–317, 1995. [436](#)
- Schröder, F., Kärcher, B., Duroure, C., Ström, J., Petzold, A., Gayet, J. F., Strauss, B., Wendling, P., and Borrmann, S.: On the transition of contrails into cirrus clouds, *Journal of the Atmospheric Sciences*, 57, 464–480, 2000. [448](#)
- 30 Sommerfeld, R. A., Conklin, M. H., and Laird, S. K.: NO adsorption on ice at low concentrations, *Journal of Colloid and Interface Science*, 149, 569–574, 1992. [433](#), [443](#), [446](#)
- Svanberg, M., Pettersson, J. B. C., and Bolton, K.: Coupled QM/MM molecular dynamics sim-

- ulations of HCl interacting with ice surfaces and water clusters - evidence of rapid ionization, *Journal of Physical Chemistry A*, 104, 5787–5798, 2000. [442](#)
- Tabazadeh, A., Toon, O. B., and Jensen, E. J.: A surface chemistry model for nonreactive trace gas adsorption on ice: Implications for nitric acid scavenging by cirrus, *Geophysical Research Letters*, 26, 2211–2214, 1999. [433](#), [447](#)
- 5 Thibert, E. and Dominé, F.: Thermodynamics and kinetics of the solid solution of HNO<sub>3</sub> in ice, *Journal of Physical Chemistry B*, 102, 4432–4439, 1998. [433](#), [447](#)
- Uras, N., Rahman, M., and Devlin, J. P.: Covalent HCl at the surface of crystalline ice at 125 K: The stable phase at submonolayer levels, *Journal of Physical Chemistry B*, 102, 9375–9377, 1998. [443](#)
- 10 Uras, N., Buch, V., and Devlin, J. P.: Hydrogen bond surface chemistry: Interaction of NH<sub>3</sub> with an ice particle, *Journal of Physical Chemistry B*, 104, 9203–9209, 2000. [443](#)
- Wang, W. C., Zhuang, Y. C., and Bojkov, R. D.: Climate implications of observed changes in ozone vertical distributions at middle and high latitudes of the northern hemisphere, *Geophysical Research Letters*, 20, 1567–1570, 1993. [433](#)
- 15 Warneck, P. and Zerbach, T.: Synthesis of peroxyacetyl nitrate in air by acetone photolysis, *Environmental Science and Technology*, 26, 74–79, 1992. [435](#)
- Winkler, D. M. and Trepte, C. E.: Laminar cirrus observed near the tropical tropopause by LITE, *Geophysical Research Letters*, 25, 3351–3354, 1998. [433](#)
- 20 Zondlo, M. A., Barone, S. B., and Tolbert, M. A.: Uptake of HNO<sub>3</sub> on ice under tropospheric conditions, *Geophysical Research Letters*, 24, 1391–1394, 1997. [442](#)

---

**Adsorption of NO<sub>y</sub>  
on ice**T. Bartels et al.

---

[Title Page](#)[Abstract](#)[Introduction](#)[Conclusions](#)[References](#)[Tables](#)[Figures](#)[◀](#)[▶](#)[◀](#)[▶](#)[Back](#)[Close](#)[Full Screen / Esc](#)[Print Version](#)[Interactive Discussion](#)

## Adsorption of NO<sub>y</sub> on ice

T. Bartels et al.

**Table 1.** Standard adsorption enthalpy and entropies of various NO<sub>y</sub> species, random error  $\sigma$ , number of measurements (in brackets) and the systematic error  $\delta_{\text{sys}}$  of  $\Delta H_{\text{ads}}^0$ . For calculation of  $\Delta S_{\text{ads}}^{01}$  a value of  $1 \text{ cm}^{-1}$  for  $A/V$  was used and for  $\Delta S_{\text{ads}}^{02}$ ,  $A$  was set to  $6.7 \times 10^{10} \text{ cm}^2$  and  $V$  to  $2.2 \times 10^4 \text{ cm}^3$

	$\Delta H_{\text{ads}}^0$ [kJ mol <sup>-1</sup> ]	$\sigma$ [kJ mol <sup>-1</sup> ]	$\delta_{\text{sys}}$ [kJ mol <sup>-1</sup> ]	$\Delta S_{\text{ads}}^{01}$ [J/(K mol)]	$\Delta S_{\text{ads}}^{02}$ [J/(K mol)]	$\sigma$ [J/(K mol)]
HNO <sub>3</sub>	-44	2.3 (4)	13	-168	-44	0.1
HONO	-32	1.7 (9)	10	-166	-42	0.1
PAN	-30	1.2 (7)	7	-169	-45	0.5
NO <sub>2</sub>	-22	1.0 (21)	6	-165	-39	0.1
NO	-20	2.6 (7)	5	-164	-40	0.2

Title Page

Abstract

Introduction

Conclusions

References

Tables

Figures

I◀

▶I

◀

▶

Back

Close

Full Screen / Esc

Print Version

Interactive Discussion

© EGS 2002

## Adsorption of NO<sub>y</sub> on ice

T. Bartels et al.

**Table 2.** Assessment of the systematic error

input value	error	influence of this error on the adsorption enthalpy					
		NO	NO <sub>2</sub>	HONO	HNO <sub>3</sub>	PAN	
experimental time	± 1 min	0.1	0.0	0.1	0.1	0.1	kJ mol <sup>-1</sup>
gas flow	± 20 cm <sup>3</sup> s <sup>-1</sup>	0.1	0.3	0.3	0.1	0.3	kJ mol <sup>-1</sup>
temperature gradient	± 0.5 K	0.1	0.1	0.1	0.2	0.1	kJ mol <sup>-1</sup>
open volume	± 300 %	1.4	1.8	1.9	2.8	1.9	kJ mol <sup>-1</sup>
surface area	± 300 %	1.1	1.6	5.2	2.2	5.2	kJ mol <sup>-1</sup>
starting temperature	+ 30 K	0.0	0.0	0.1	3.0	0.0	kJ mol <sup>-1</sup>
deposition temperature	± 10 K	1.8	2.7	2.5	4.2	2.8	kJ mol <sup>-1</sup>
molar mass	+ 1 g mol <sup>-1</sup>	0.0	0.0	0.0	0.0	0.0	kJ mol <sup>-1</sup>

Title Page

Abstract

Introduction

Conclusions

References

Tables

Figures

I◀

▶I

◀

▶

Back

Close

Full Screen / Esc

Print Version

Interactive Discussion

© EGS 2002



**Table 3.** Partitioning coefficient of nitrogen oxides between ice and air under different atmospheric conditions. See text for explanation and references

		temperature [K]	ice area [cm <sup>2</sup> cm <sup>-3</sup> ]	partition coefficient [-]
contrails	NO	213	1×10 <sup>-2</sup>	2×10 <sup>-6</sup>
	NO <sub>2</sub>	213	1×10 <sup>-2</sup>	6×10 <sup>-6</sup>
	HONO	213	1×10 <sup>-2</sup>	2×10 <sup>-3</sup>
	PAN	213	1×10 <sup>-2</sup>	3×10 <sup>-4</sup>
	HNO <sub>3</sub>	213	1×10 <sup>-2</sup>	1
cirrus clouds	NO	213	3×10 <sup>-3</sup>	7×10 <sup>-7</sup>
	NO <sub>2</sub>	213	3×10 <sup>-3</sup>	2×10 <sup>-6</sup>
	HONO	213	3×10 <sup>-3</sup>	5×10 <sup>-4</sup>
	PAN	213	3×10 <sup>-3</sup>	1×10 <sup>-4</sup>
	HNO <sub>3</sub>	213	3×10 <sup>-3</sup>	3×10 <sup>-1</sup>
snow pack (polar zone)	NO	246	20	1×10 <sup>-3</sup>
	NO <sub>2</sub>	246	20	3×10 <sup>-3</sup>
	HONO	246	20	3×10 <sup>-1</sup>
	PAN	246	20	8×10 <sup>-2</sup>
	HNO <sub>3</sub>	246	20	9×10 <sup>+1</sup>
snow pack (temperate zone)	NO	268	70	2×10 <sup>-3</sup>
	NO <sub>2</sub>	268	70	3×10 <sup>-3</sup>
	HONO	268	70	3×10 <sup>-1</sup>
	PAN	268	70	7×10 <sup>-2</sup>
	HNO <sub>3</sub>	268	70	4×10 <sup>+1</sup>

## Adsorption of NO<sub>y</sub> on ice

T. Bartels et al.

Title Page

Abstract

Introduction

Conclusions

References

Tables

Figures

◀

▶

◀

▶

Back

Close

Full Screen / Esc

Print Version

Interactive Discussion

© EGS 2002

Adsorption of  $\text{NO}_y$   
on ice

T. Bartels et al.

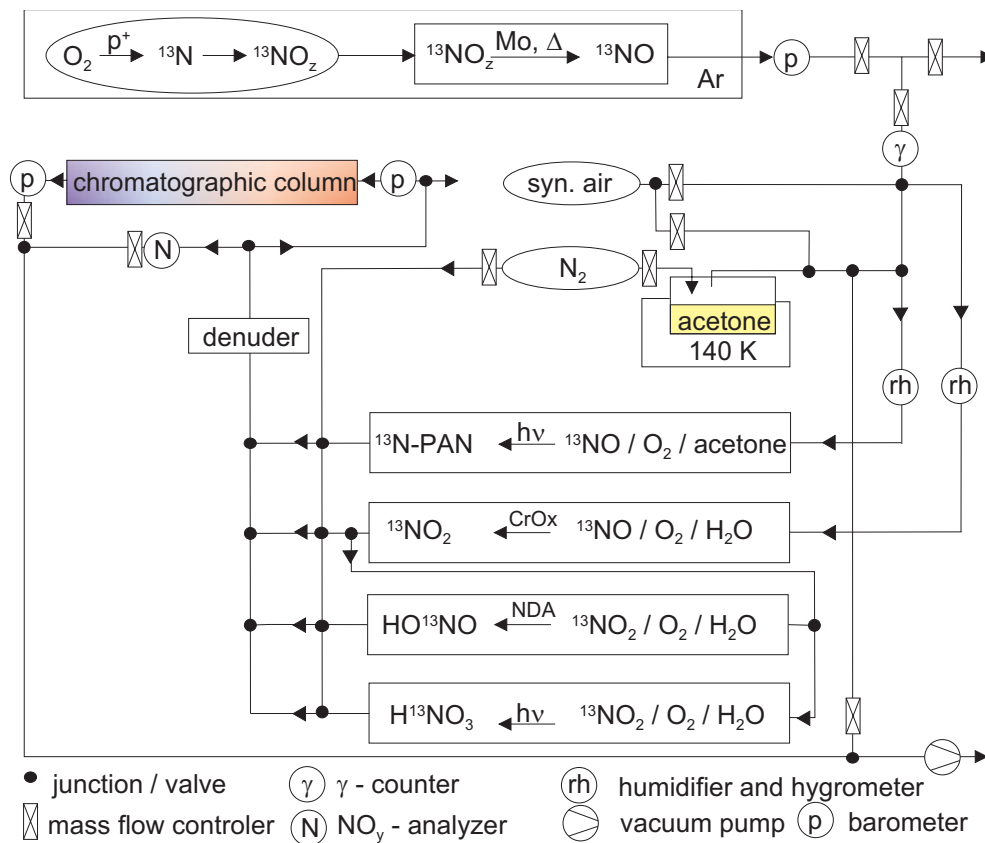


**Fig. 1.** Experimental setup: gas target to produce  $^{13}\text{N}$ , photolysis cells to oxidise the nitrogen oxides, and chromatographic column.

Title Page

Abstract

Introduction

Conclusions

References

Tables

Figures

◀

▶

◀

▶

Back

Close

Full Screen / Esc

Print Version

Interactive Discussion

© EGS 2002

Adsorption of  $\text{NO}_y$   
on ice

T. Bartels et al.

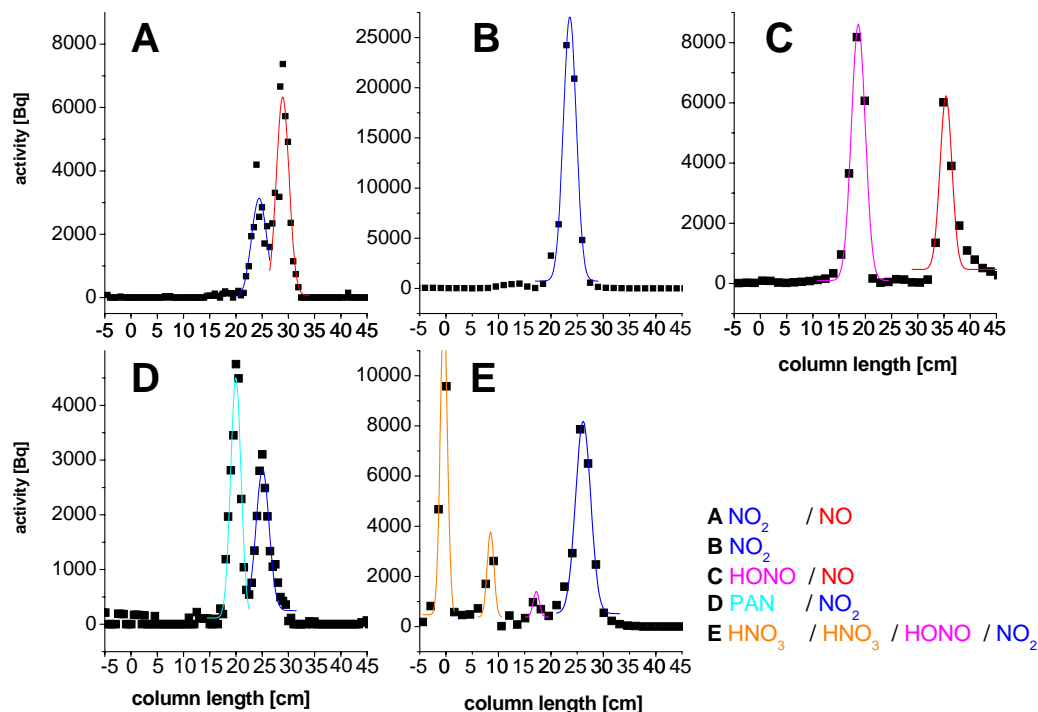


**Fig. 2.** Distribution of different nitrogen oxide species in columns packed with ice spheres at different experimental settings. Zero column length denotes the beginning of the ice spheres in the column. The activity is a measure for concentration of  $\text{NO}_y$  species along the column. The spontaneous signals visible at the column entrance in chromatogram D are due to detector noise, and their decreasing relative contribution derives from the calculation of the activity based on the observed counts.

Title Page

Abstract

Introduction

Conclusions

References

Tables

Figures

◀

▶

◀

▶

Back

Close

Full Screen / Esc

Print Version

Interactive Discussion

© EGS 2002

## Adsorption of NO<sub>y</sub> on ice

T. Bartels et al.

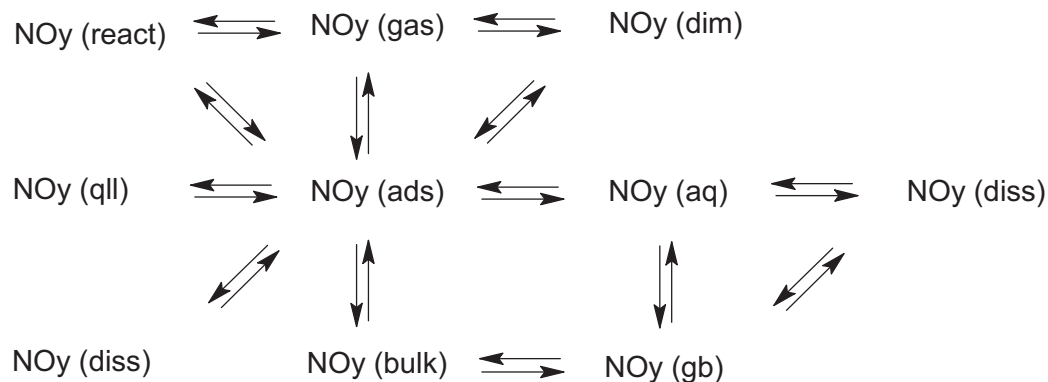


**Fig. 3.** Overview of equilibria of nitrogen oxides in the gas and ice phase, such as dimerisation (dim), e.g.  $\text{NO}_2 \rightleftharpoons \text{N}_2\text{O}_4$ ; adsorption (ads); reaction (react), e.g.  $\text{NO}_2 + \text{NO} \rightleftharpoons \text{N}_2\text{O}_3$ ; solvation into the quasi-liquid layer (qll), bulk or grain boundaries (gb); formation of encapsulated hydrates (aq); and dissociation (diss), e.g. of  $\text{HNO}_2$  and  $\text{HNO}_3$ .

Title Page

Abstract

Introduction

Conclusions

References

Tables

Figures

◀

▶

◀

▶

Back

Close

Full Screen / Esc

Print Version

Interactive Discussion

© EGS 2002

Adsorption of  $\text{NO}_y$   
on ice

T. Bartels et al.

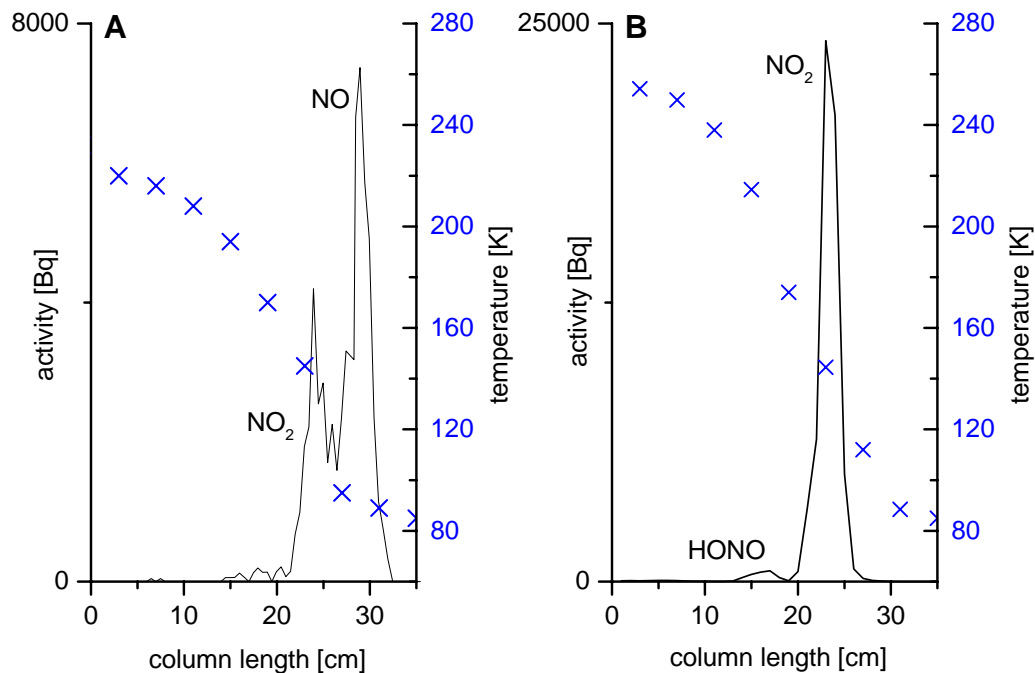


**Fig. 4.** Comparison of two chromatograms at different experimental settings. The activity is given on the left axis (solid line) and the temperature along the column at the right axis (crosses). In experiment A the temperature at column entrance was too low for a quasi-liquid layer to form, whereas in chromatogram B a quasi-liquid layer might have evolved. Note that the two  $\text{NO}_2$  peaks should be compared; the NO in experiment A was added on purpose, without any relation to this comparison.

[Title Page](#)[Abstract](#)[Introduction](#)[Conclusions](#)[References](#)[Tables](#)[Figures](#)[◀](#)[▶](#)[◀](#)[▶](#)[Back](#)[Close](#)[Full Screen / Esc](#)[Print Version](#)[Interactive Discussion](#)

© EGS 2002

Adsorption of  $\text{NO}_y$   
on ice

T. Bartels et al.

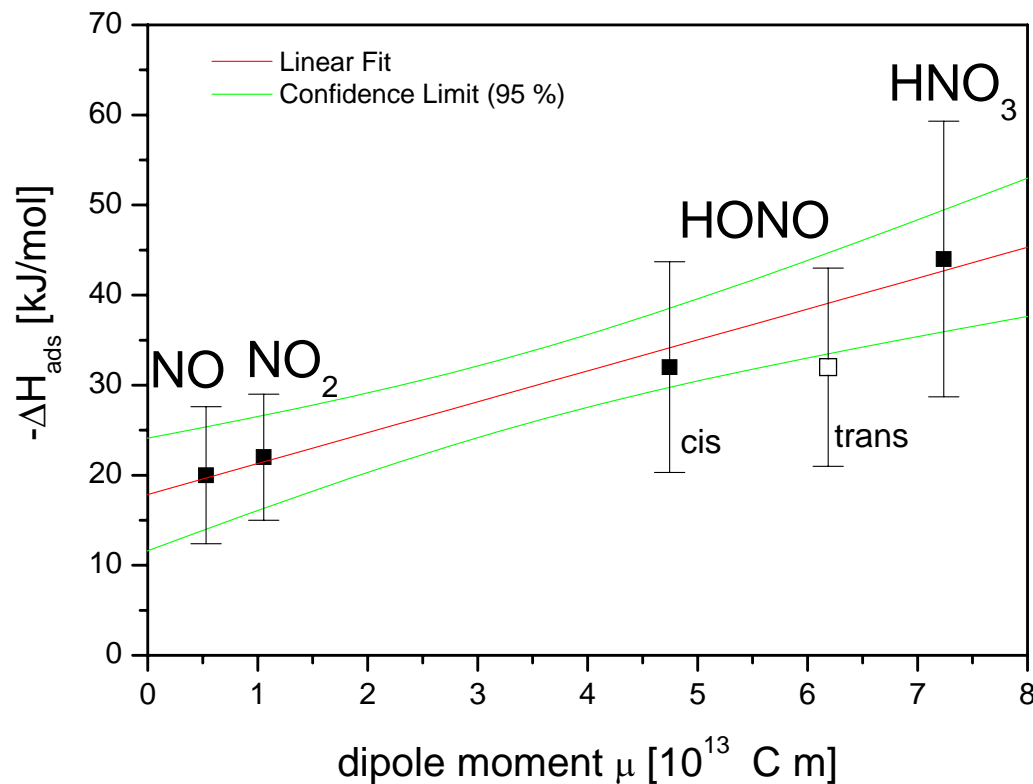


**Fig. 5.** Correlation of dipole moment (Lide, 2001–2002) and the experimentally found adsorption enthalpy for  $\text{NO}$ ,  $\text{NO}_2$  and  $\text{HNO}_3$ .

[Title Page](#)[Abstract](#)[Introduction](#)[Conclusions](#)[References](#)[Tables](#)[Figures](#)[◀](#)[▶](#)[◀](#)[▶](#)[Back](#)[Close](#)[Full Screen / Esc](#)[Print Version](#)[Interactive Discussion](#)

© EGS 2002